University of Wrocław
Faculty of Physics and Astronomy
Institute of Experimental Physics

Tomasz Greczyło

The Use of Digital Techniques in an Investigation of Coupled Oscillations of a Wilberforce Pendulum

The thesis written in
Division of Physics Teaching

Promotor:

prof. Ewa Dębowska

Amsterdam / Wrocław 2001

The thesis written in academic year 2000/2001 during a study in frame of Socrates/Erasmus program at Amstel Institute of University of Amsterdam

Contents

I. Preface

Abstract

In this paper phases of work completed before and during making measurements on video clips and their results are presented. It includes preparation of experiments, recording and processing video clips, acquiring and analyzing results. Data Video mode of Coach 5 was used to monitor motion of Wilberforce pendulum and to measure changes of both its coordinates: vertical displacement of the bob and its rotational angle over time. The experiments were carried out with different combinations of initial conditions and recorded from two camera perspectives. Fourier analysis of the results confirm the presence of two frequencies corresponding to normal modes. The results of measurements also show beats between the normal modes and each of them separately and allow verifying the equations of Wilberforce pendulum motion.

Streszczenie

Niniejsza praca prezentuje zastosowanie technik cyfrowych do badania ruchu wahadła Wilberforce'a oraz przedstawia wyniki pomiarów wideo drgań podłużnych i drgań skrętnych (torsyjnych) tego wahadła.

Autor opisuje poszczególne etapy pracy związanej z tym rodzajem pomiarów tj. przygotowanie eksperymentu, jego rejestrację za pomocą cyfrowej kamery wideo, obróbkę filmów wideo, pomiary wideo z zastosowaniem programu Coach 5 oraz analizę FFT (szybka transformata Fouriera) wyników z użyciem arkusza kalkulacyjnego Excel. Eksperymenty zostały przeprowadzone dla przypadku rezonansu drgań podłużnych i skrętnych, dla różnych kombinacji warunków początkowych: wydłużenia sprężyny i skręcenia dysku wahadła. Wyniki umożliwiły znalezienie wartości częstotliwości własnych układu, obserwację dudnień związanych z występowaniem dwóch nieznacznie różniących się częstotliwości oraz każdego z dwóch modów oddzielnie, a także obliczenie stałej sprzężenia.

W pierwszym rozdziale pracy prezentowane są zagadnienia teoretyczne niezbędne do analitycznego opisu ruchu wahadła Wilberforca, które obejmują:

- podstawowe własności mechaniczne materiałów,
- drgania torsyjne,
- wpływ masy sprężyny na statyczne i dynamiczne charakterystyki wahadła sprężynowego,
- ścinanie i zginanie sprężyny spiralnej,
- wahadła sprzężone, mody oraz dudnienia,
- wahadło Wilberforce'a,
- analizę Fouriera.

Rozdział drugi opisuje proces tworzenia cyfrowych filmów wideo, ich obróbkę, przygotowanie do pomiarów oraz analizę wyników. W tej części pracy szczególną uwagę poświęcono programom komputerowym użytym do:

- obróbki filmów cyfrowych – Adobe Premierer$^®$,
- pomiarów wideo – Coach 5,
- obróbki, prezentacji i analizy danych – MS Excel$^®$.

Rozdział trzeci zawiera opis badanego wahadła Wilberforca, przebieg doświadczeń oraz sposób obróbki danych. Otrzymane wyniki są w tej części przedstawione w tabelach i na wykresach.

Zastosowanie techniki cyfrowej obróbki obrazu oraz rejestracji danych pozwoliło na wizualizację podłużnych i torsyjnych oscylacji wahadła Wilberforce'a; zgodnie ze stanem mojej wiedzy jest to pierwsza wizualizacja tego typu. Zebrane wyniki zostały porównane z opublikowanymi w [1] i pozwoliły zweryfikować równania opisujące ruch wahadła Wilberforca oraz obliczyć wartość stałej sprzężenia.

Praca zawiera także sugestie jak usprawnić proces otrzymywania wyników podczas pomiarów wideo oraz jak zwiększyć ich dokładność, by mogły być w przyszłości częściej wykorzystywane. Do pracy załączone są dwie płyty CD zawierające cyfrowe filmy wideo, na których autor dokonał pomiarów wideo.

II. Introduction

Aims of the Thesis

Using digital techniques for investigations in natural phenomena is a modern method to develop many interesting aspects in physics as well as in other disciplines. The use of digital cameras, hardware and software to produce a movie and powerful programs to take measurements from it opens new ways to explore a variety of scientific subjects. Also developing of electronic devices and significant improvement of existing method of digital signal processing encourage us to take their advantages in (re)investigation of some important features of motion and/or many other aspects that are related to it.

A number of computer programs such as Coach 5, VideoPoint, VideoGraph, Vidshell can be used to make measurements of the position of an object whose motion has been covered and produced as a video clip. Information about x- and y-axis are usually gained from certain frames of a scaled and made with known frame rate digital movie.

The present thesis is aimed to introduce video measurement with its useful tools that can be used in science exploration. As an example of such a program Video Measurement of Coach 5 was chosen.

The author would like to illustrate and describe in details the use of digital techniques (video production, video measurement) with a scientific example of Wilberforce pendulum motion. Therefore the preparation of experiments, processing, measuring and analysing phases of work are described. He believes that obtained results allow making experimental verification of this coupled pendulum motion. The paper shows that it is possible to investigate, with sufficient accuracy, the time dependence of the vertical displacement and the rotational angle of the pendulum, with use of Coach 5 Video Measurement. It will be, according to his knowledge, first measurement of the rotation angle of Wilberforce pendulum bob and the second visualisation of its motion.

Obtained results are compared with those described in [1] where experimental verification of the important features of the motion of the Wilberforce pendulum and results of the experiment, during which longitudinal displacement of its bob is measured with a ultrasound sensor, are presented.

The author also presents verification of motion equations of Wilberforce pendulum and calculates the value of a coupling constant for measured device.

III. Substance

Chapter 1. Mechanics of Deformable Bodies

1.1. Mechanical Properties of Materials

When external forces or moments of forces are applied to a solid body its shape and/or volume can be changed. If these forces are not large the body will return to its original shape and volume immediately after the distorting forces are removed. This property of a solid body is called elasticity.

If applied forces are sufficiently large the solid body can be permanently stretched. This is called plasticity.

The way in which forces are applied determines the elastic behaviour of a solid body. One can specify three such ways, namely: longitudinal, volumetric and shearing forces.

First the case when a parallelepiped block of uniform cross-sectional area S is under compression due to equal and opposite forces applied along its z-axis will be considered. Figure 1.1.1 that was taken from [2] shows such a situation. The problem can be

Figure 1.1.1. A parallelepiped solid block of elastic material under tension

described with analogy if a tension force is applied to increase the length of the parallelepiped in the z-direction. In both cases the same effect is observed.
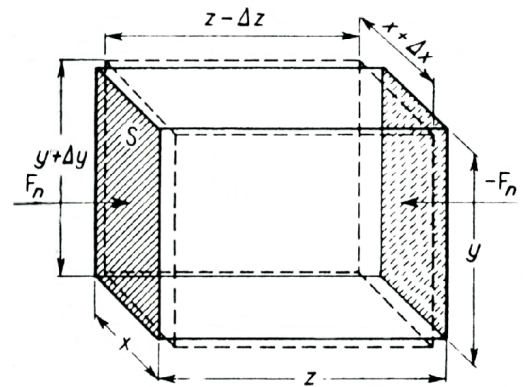
When the compression force is increased from F_n to $F_n+\Delta F$, the initial length of the parallelepiped z will change to $z-\Delta z$. Observing dependence of the frictional change in length (so called longitudinal strain defined as $\Delta z/z$) on the force per unit area (so called longitudinal stress defined as $\Delta F/S$) one can see that as long as force is not too large $\Delta z/z$ is proportional to $\Delta F/S$. That is:

$$\frac{\Delta z}{z} \propto \frac{\Delta F}{S} \qquad \text{or} \qquad \frac{\Delta F}{S} = E\frac{\Delta z}{z} \qquad\qquad (1.1.1)$$

where E is constant of proportionality with unit [N/m^2] and characterises the material from which the body is made.

8

The constant is called the Young modulus of the material and is defined by:

$$E \equiv \frac{z}{S} \cdot \frac{dF}{dz}$$

(1.1.2)

Examples of values of the Young modulus for a number of solids are given in a table 1.1.1 [3].

Table 1.1.1. Elastic constants of some common substances at 20°C

Substance	Young modulus N·m^{-2}	Shear modulus N·m^{-2}	bulk modulus N·m^{-2}
aluminium	$7,0 \cdot 10^{10}$	$2,6 \cdot 10^{10}$	$7,6 \cdot 10^{10}$
brass	$1,0 \cdot 10^{11\#}$	$4,0 \cdot 10^{10}$	$1,0 \cdot 10^{11\#}$
copper	$1,3 \cdot 10^{11}$	$4,8 \cdot 10^{10}$	$1,4 \cdot 10^{11}$
gold	$7,8 \cdot 10^{10}$	$2,7 \cdot 10^{10}$	$2,2 \cdot 10^{11}$
steel (mild)	$2,1 \cdot 10^{11}$	$8,2 \cdot 10^{10}$	$1,7 \cdot 10^{11}$
# denotes approximate values			

In a case of permanent stretching the relationship between stress and strain is no longer linear. The forces produce the dislocation and process can not be completely reversed. The point at which the behaviour of a solid becomes non-linear and non-reversible is called the elastic limit.

The second consideration of elastic properties of solid deals with volumetric stress. In this case forces that produce the extension of a solid are applied to the body equally in all directions. It causes a change in volume. Such a situation for a cube is shown in figure 1.1.2. that was found in [3]. All forces ΔF are applied perpendicularly to all six faces and produce a volume change ΔV.
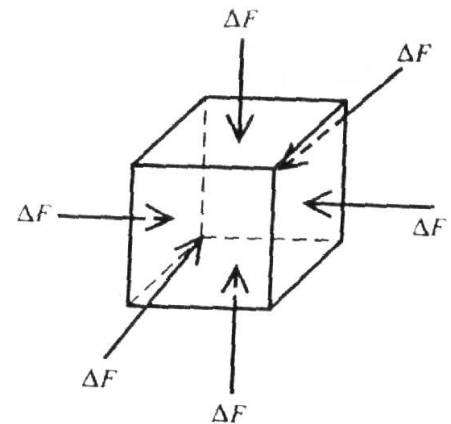

Figure 1.1.2. A cubical solid block under a volumetric stress

Assuming that the elastic limit is not exceeded one can see that the volumetric strain $\Delta V/V$ is proportional to the volumetric stress $\Delta F/S$, where S is the area of one face of a cube. It can be written as:

$$\frac{\Delta V}{V} \propto \frac{\Delta F}{S} \quad \text{or} \quad \frac{\Delta F}{S} = -K \frac{\Delta V}{V}$$

(1.1.3)

where K is a constant of proportionality with unit [N/m^2] and called the bulk modulus. The constant is a characteristic of the material under study.

The bulk modulus is defined as:

$$K \equiv -\frac{V}{S} \cdot \frac{dF}{dV} \qquad\qquad (1.1.4)$$

The minus sign is included so that K is positive because dF/dV is always negative (an increase of applied force causes a decrease in volume). Examples of the bulk modulus for a number of materials are presented in table 1.1.1.

As a last case the situation of a shearing stress will be considered. When equal and opposite forces are applied to opposite faces of a solid block it will act showing different elastic behaviour. Assume that the elastic limit is not exceeded and the cuboid returns to its original shape when the forces are removed. To invoke this effect one can consider the distortion of a solid cuboid by equal and opposite forces F_s that are applied tangentially to opposite faces of a cuboid. The situation is shown in figure 1.1.3, which was taken from [2].
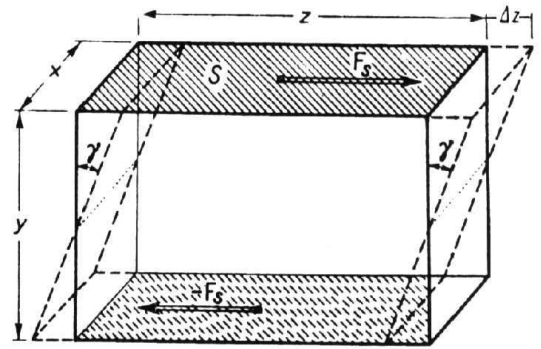

Figure 1.1.3. A solid parallelepiped block under a shearing stress

The net effect of such forces is that the rectangular faces of the parallelepiped in the plane of he applied forces become parallelogram. A force per unit area applied tangentially is called a shearing stress. The corresponding shearing strain is defined (for a small Δz) as $\Delta z/y$ or $\Delta \gamma$. Taking to account recent assumption one can see that the stress is proportional to strain:

$$\Delta \gamma \propto \frac{\Delta F}{S} \qquad \text{or} \qquad \frac{\Delta F}{S} = G \cdot \Delta \gamma \qquad\qquad (1.1.5)$$

where G is a constant of proportionality with unit [N/m^2].

The constant is characteristic of the material called a shear modulus and defined as:

$$G \equiv -\frac{1}{S} \cdot \frac{dF}{d\gamma} \qquad\qquad (1.1.6)$$

Examples of the shear modulus for a number of materials are given in table 1.1.1.

As it is shown in figure 1.1.1 the change in length z of a parallelepiped solid block in particular and bodies of different shape under a shearing stress in general is accompanying by changes of other dimensions - x and y. For isotropic bodies the following equation is valid:

$$\frac{\Delta x}{x} = \frac{\Delta y}{y} = \nu \frac{\Delta z}{z} \qquad (1.1.6)$$

where ν is a constant of proportionality called Poisson's ratio.

The constant has no unit and for majority of materials is enclosed between 0,2 and 0,4. When during deformation the change in volume does not take place ν is equal to 0,5. The presented constants satisfy the equation:

$$G = \frac{E}{2(1+\nu)} \qquad (1.1.7)$$

1.2. Tortional oscillation

When rigid body is suspended from a vertical length of wire (or a rod) that is attached to a fixed point and a small twist has been given to it and then released from rest one can observe torsional oscillation.

If angular displacement is θ and restoring torque is proportional to it, $T = -c\theta$, one can write an equation:

$$T = \frac{dL}{dt} = \frac{d}{dt}(I\omega) = I\frac{d\omega}{dt} = I\frac{d^2\theta}{dt^2} = -c\theta \qquad (1.2.1)$$

where L is an angular momentum, ω indicates angular velocity and I represents moment of inertia of the rigid body about the axis of the wire or rod. Looking at a last part of the equation one gets:

$$I\frac{d^2\theta}{dt^2} + c\theta = 0 \qquad (1.2.2)$$

This is an equation of a simple harmonic oscillator. The rigid body executes simple harmonic oscillation about wire's axis with a period:

$$T = 2\pi \cdot \sqrt{\frac{I}{c}} \qquad (1.2.3)$$

A well-known example of a simple harmonic oscillator is a spring oscillator with a mass m attached to a helical spring with an elastic constant k. In this case the equation determining a period has a form:

$$T' = 2\pi \cdot \sqrt{\frac{m}{k}} \qquad (1.2.4)$$

1.3. Influence of a Mass of a Spring on its Static and Dynamic

Usually calculations of an elongation or an oscillation period of a spring pendulum are done with an assumption that the spring is massless. In reality this mass affects pendulum motion.

As in [4] and [5] first a static case will be discussed. To find the solution one assumes that l is the unloaded spring length, m represents its mass and k is an elastic constant of a spring.

The elongation of the unit of spring due to a force $\Delta G = k \cdot \Delta l$ is:

$$\Delta l' = \frac{\Delta l}{l} = \frac{\Delta G}{lk} \qquad (1.3.1)$$

Therefore portion of the length dz suffers an elongation:

$$\Delta(dz) = dz \Delta l' = \frac{\Delta G}{lk} dz \qquad (1.3.2)$$

Since:

$$\Delta(dz) = \frac{\Delta G}{k'} \qquad (1.3.3)$$

one can consider an elastic constant of a small portion of a spring length dz as:

$$k' = \frac{kl}{dz} \qquad (1.3.4)$$

When a mass M is placed at the end of the spring the load acting to the element between z and $z+dz$ becomes equal to:

$$G^{`}=(M+m\cdot(l\text{-}z)/l)\cdot g \tag{1.3.5}$$

and it suffers an elongation:

$$\Delta(dz) = \frac{G'}{k'} = \frac{M + m(l-z)/l}{kl} g \cdot dz \tag{1.3.6}$$

Integrating according to z from $z=0$ to $z=l$ one gets the total elongation of the spring:

$$\Delta l = \int_{0}^{l} \Delta \cdot dz = \frac{(M + m/2) \cdot g}{k} \tag{1.3.7}$$

It leads to conclusion that in static conditions the elongation suffered by a non-null mass spring is equivalent to supposing the spring is massless and adding a mass equal to half the mass of the spring to the bob's mass M at its end.

Elaborating a dynamic case one starts with assumption that mass M has been placed at the end of the spring, displaced from equilibrium position and then released. So, oscillations occur and the element of the spring dz suffers a deformation du that is produced by the force:

$$F = k'du = \frac{kl}{dz}\frac{\partial u}{\partial z}dz = kl\frac{\partial u}{\partial z} \tag{1.3.8}$$

besides:

$$dF = \frac{\partial F}{\partial z}dz \qquad dm = \frac{m}{l}dz \tag{1.3.9}$$

According to the equation:

$$dF = dm\frac{\partial^2 u}{\partial t^2} \tag{1.3.10}$$

one gets:

$$\frac{\partial F}{\partial z}dz = \frac{m}{l}\frac{\partial^2 u}{\partial t^2}dz \tag{1.3.11}$$

hence:

$$kl\frac{d^2 u}{\partial z^2} = \frac{m}{l}\frac{\partial^2 u}{\partial t^2} \tag{1.3.12}$$

This is the equation of a wave whose velocity is:

$$V = \sqrt{\frac{kl^2}{m}} \qquad (1.3.13)$$

To portrait the elongation u of the abscissa of a point z and the force one can write:

$$u(z,t) = A \cdot sin(\beta \cdot z + \varphi) \cdot sin(\omega t + \alpha) \qquad (1.3.14)$$

$$F(z,t) = kl\frac{\partial u}{\partial z} \qquad (1.3.15)$$

where ω is an angular frequency and $\beta = \omega/V$ and α, β are phase angles. The boundary conditions at the upper and lower ends are:

$$z = 0; \; u(0,t) = 0 \qquad (1.3.16a)$$

$$z = l; \; -F(l,t) = M\frac{\partial^2 u}{\partial t^2} \qquad (1.3.16b)$$

which, when entered in to (1.3.14) and (1.3.15), with assumption $\varphi = 0$, gives:

$$u(z,t) = A \cdot sin(\beta \cdot z)sin(\omega t + \alpha) \qquad (1.3.17)$$

$$F(z,t) = klA\beta \cdot cos(\beta z) \cdot sin(\omega t + \alpha) \qquad (1.3.18)$$

Therefore:

$$F(l,t) = M\frac{\partial^2 u(l,t)}{\partial t^2} = M\omega^2 A \sin \beta l \sin(\omega t + \alpha) \qquad (1.3.19)$$

hence,

$$\omega^2 = (kl\beta)/(M \cdot tg(\beta l)) \qquad (1.3.20)$$

which, together with (1.3.13) and definition of β, gives an equation :

$$tg(\beta l) = (M/m)\beta l \qquad (1.3.21)$$

This allows to conclude that for each ratio between the mass M and spring mass m there is a set of solutions that correspond to the different modes of vibration of a system. As the relation M/m grows the solutions tend to the value $(\beta l)_n=(n-1)\pi$, where n is the order number of a harmonics. For n=1 there is a fundamental vibration. When the mass of a spring m is extremely small in comparison to M the value of fundamental (βl) tends to zero and equation becomes the classical formula of a harmonic oscillator – formula (1.2.4). In any other case, one can write:

$$\omega^2=k/(M+m/D) \tag{1.3.22}$$

where m/D is a portion of whole mass of a spring m (D is an real number).
When combined with (1.3.20) one obtains:

$$D = \frac{m}{M}\left[\frac{\beta l}{(tg(\beta l) - \beta l)}\right] \tag{1.3.23}$$

For $m/M \to O$, $D = 3$ and for $m/M \to \infty$, $D = \pi^2/2 \approx 2,467$.

For a spring whose length is small compared to ¼ of the wavelength of the characteristic vibration wavelength an assumption that the displacements of the elements of the spring are proportional to z can be made. In such a case, the whole system energy is given by:

$$E = \tfrac{1}{2}(M\omega^2 A^2)+\frac{\omega^2}{2}\int_0^l\left(\frac{Az}{l}\right)^2 dm = \tfrac{1}{2}(M\omega^2 A^2)+\frac{A^2 m\omega^2}{2l^3}\int_0^l z^2 dz =\frac{1}{2}\left[\omega^2 A^2\left(M +\frac{m}{3}\right)\right] \tag{1.3.24}$$

where M is a mass of a bob and A an amplitude of its displacement from equilibrium position.

It leads to conclusion that in dynamic conditions one has to add a mass equal to one-third of the mass of the spring to the bob's mass M at its end in order to obtain the same energy.

1.4. Torsion and Bending of a Helical Spring

One can obtain a helical spring by winding a few layers of a thin wire on a circular cylinder and then removing the mandrel. Such a spring is presented in figure 1.4.1a. that was found in [2]. The wire in the diagram has been drawn with a ribbon shape to indicate behaviour of the spring when force F or moment M are applied, but the behaviour is independent of the actual shape.
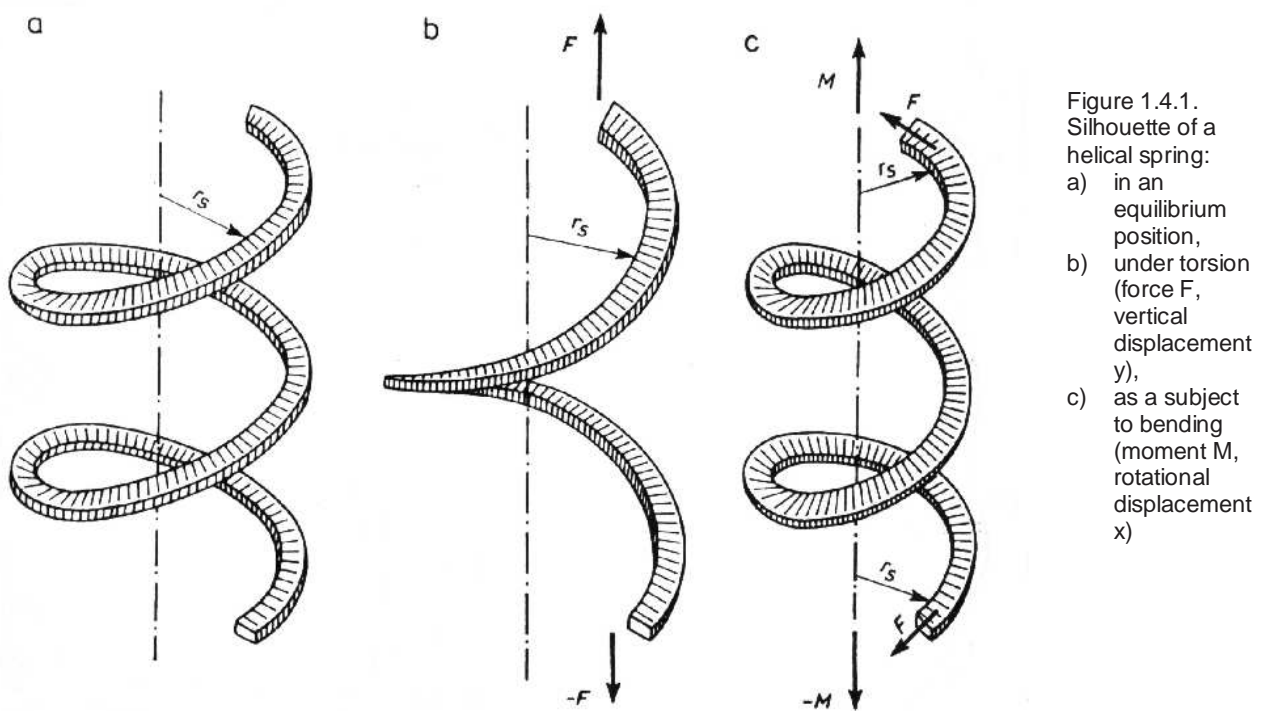

Figure 1.4.1. Silhouette of a helical spring:
a) in an equilibrium position,
b) under torsion (force F, vertical displacement y),
c) as a subject to bending (moment M, rotational displacement x)

If one end of such a spring is attached to a fixed point and the other end loaded with a puck-shaped bob one obtains a system to be studied. When the bob's weight is small so that the resulting pitch of the spring is small comparing to the radius of the cylinder r_s one can observe a small load acting along the axis of the spring which results in a slightly increased pitch and a corresponding lengthening of the spring. This kind of loading is accompanied by torsion of the wire and illustrated in figure 1.4.1b.

When the bob is turned in its own plane the pitch remains essentially unchanged and the spring yields to the torque by a slight diminution of the cylinder radius r_s. In this case, as shown in figure 1.4.1c the wire is bent.

In torsion the individual cross-sections of the wire are loaded by a torque about the polar axis while in bending the moment acts about on an axis in the plane of the cross-section.

The load F acting along the cylinder axis has the moment $F \cdot r_s$ about the centre of the cross-section, the so called torsional moment M_t, since its axial vector is normal to the cross-section. In the case of bending the moment of force F' acts upon the bob whose diameter has been assumed as $2r_s$. This moment has a character of a bending moment M_b since its axial vector coincides with the cylinder axis and can be transferred parallel to itself to the centre of the marled cross-section. In the loading there will be shear stresses in the plane of the cross-section which increase proportionally to the distance from the wire axis and will be denoted by τ. Therefore one has:

$$\int r \cdot \tau \cdot df = M_t \tag{1.4.1}$$

where df is the area element of the cross section of a wire.

In the loading normal stresses σ act upon the cross-section and they are proportional to the distance y which can be expressed as:

$$\int y \cdot \sigma \cdot df = M_b \tag{1.4.2}$$

The entire torsion energy E_T for the helical spring is equal to:

$$E_T = \frac{M_t^2 l}{2GJ_P} = \frac{F^2 r_s^2 l}{2GJ_P} \tag{1.4.3}$$

where l represents a length of a spring, G is a shear modulus and J_p denotes a polar moment of inertia of the cross-section which in the case of circular area is twice the equatorial moment of inertia [6].

The entire bending energy contained in the spring is:

$$E_B = \frac{M_b^2 l}{2EI} = \frac{F'^2 r_s^2 l}{2EI} \tag{1.4.4}$$

where I represents the equatorial moment of inertia and E is a Young modulus [6].

The expressions (1.4.3) and (1.4.4) represent the energy content of the spring in an elastic deformation in which the spring passes through a sequence of states of equilibrium. These formulas can be compare with equations of the mechanical work performed along the path y and x when the load F and moment M increase gradually from 0 to their final value, which are:

$$W_T = \frac{Fy}{2} \qquad W_B = \frac{F'x}{2} \tag{1.4.5}$$

These lead to the determination of displacements x and y to be:

$$y = \frac{r_s^2 l}{GJ_p} F \qquad x = \frac{r_s^2 l}{EI} F' \tag{1.4.6}$$

According to the above and denoting m to represent mass of bob, L its moment of inertia and m' the mass of spring itself one gets the equations of the free torsional and bending oscillations as:

$$\frac{d^2 y}{dt^2} + \frac{GJ_P}{(m + \frac{1}{3}m')r_s^2 l} y = 0 \tag{1.4.7}$$

$$\frac{d^2 x}{dt^2} + \frac{EI}{(L + \frac{1}{3}m'r_s^2)r_s^2 l} x = 0 \tag{1.4.8}$$

The associated circular frequencies are:

$$\omega_T = \sqrt{\frac{GJ_P}{(m + \frac{1}{3}m')r_s^2 l}} \qquad \omega_B = \sqrt{\frac{EI}{(L + \frac{1}{3}m'r_s^2)r_s^2 l}} \tag{1.4.9}$$

When they are equal or almost so resonance occurs and the behaviour of a spring is very sensitive to small changes of the parameters involved. Then the present theory is no longer sufficient and indeed one has two coupled modes of oscillations.

Taking into account F and F' as inertial forces:

$$F = -m\frac{d^2 y}{dt^2} \qquad F' = -(m + \frac{1}{3}m')\frac{d^2 x}{dt^2} \tag{1.4.10}$$

the following equations that describe coupled oscillation of the spring are obtained:

$$\frac{d^2 y}{dt^2} + \omega_T^2 (y - kx) = 0 \tag{1.4.11}$$

$$\frac{d^2 x}{dt^2} + \omega_B^2 (x - ky) = 0 \tag{1.4.12}$$

1.5. Two Coupled Pendulums, Normal Modes and Beats

When observing the motion of coupled pendulums shown in a figure 1.5.1a-c, that was taken from [7] a several different aspects of its behaviour, which depend of initial conditions of a device, can be noticed.
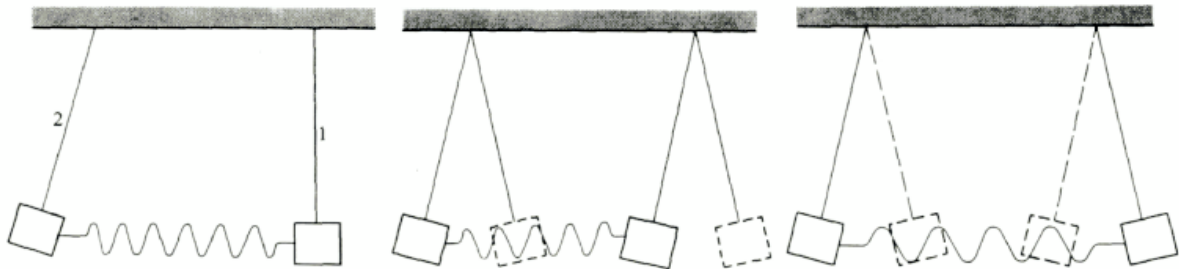

Figure 1.5.1. Two pendulums coupled with a spring: a) 1 held at rest and 2 displaced to perform oscillations, b) oscillations in phase, c) oscillations in anti-phase

When pendulum 1 is held at rest and pendulum 2 let to perform a few oscillations one observes that the first pendulum gradually begins to swing with increasing amplitude while the amplitude of the second pendulum diminishes. After certain amount of time the pendulum initially held at rest is swinging with the amplitude of the second pendulum at the beginning of its motion. Situation repeats and pendulum 1 loses its energy to pendulum 2. One can easily notice two periods, the one of oscillation of each pendulum and the second of the wandering energy from one pendulum to the other.

When both pendulums start their oscillation together and in phase as it is shown in figure 1.5.1b the exchange of energy is not observed. If it was not for frictional losses or transfer of energy into the surroundings the oscillations would go undamped.

The diminishing of amplitude is also not noticeable for the motion of a system when the pendulums are started together but in anti-phase (situation in figure 1.5.1c). This motion is

characterised by a single frequency. Every part of a system maintains a constant phase relationship with respect to every other part. Such oscillations are called natural (or normal) modes.

The oscillation frequency f_{sym} of the pendulums oscillating in phase is practically the same as that of free pendulum because the spring is hardly neither contracted nor extended during motion. This mode is also called a symmetric mode.

When pendulums oscillate in anti-phase the spring acts at every time and similarly to gravity force tends to restore equilibrium. Situation can be then described as motion of a pendulum with stronger gravitational force – bigger value of gravitational constant g.

Therefore the frequency of the second mode, the so called anti-symmetric mode, is higher then that of the first:

$$f_{asym} > f_{sym}.$$

Every free oscillation of the system can be regarded as a superposition of normal modes. Some examples are presented in figure 1.5.2.

As it has been already mentioned two modes do not proceed with the same frequency so time required for a full oscillation is: $T_{sym} > T_{asym}$. In time T_{asym} one mode makes one full oscillation and has T_{sym}-T_{asym} to cover a part of the next oscillation.

Figure 1.5.2. Examples of superposition of normal modes

So:

$$\frac{2\pi}{T_{asym}} = \frac{x}{T_{sym} - T_{asym}} \qquad x = \frac{2\pi(T_{sym} - T_{asym})}{T_{asym}} = \frac{2\pi}{f_{sym}}(f_{asym} - f_{sym}) \qquad (1.5.1)$$

Since during each oscillation the gain is x one gets n oscillations of the first mode when the second has gained the amount π in phase:

$$n = \frac{\pi}{x} = \frac{f_{sym}}{2(f_{asym} - f_{sym})} \qquad (1.5.2)$$
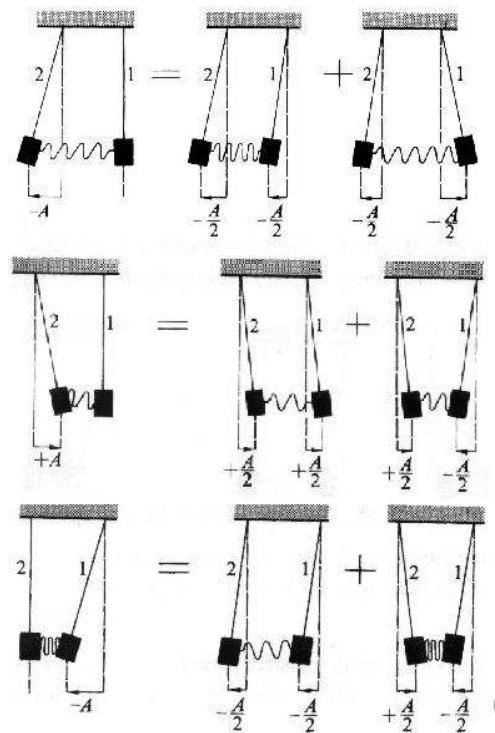
When n is integral or a half-integral number the transfer of energy from pendulum 2 to pendulum 1 will be completed.

The total energy of a pendulum for small angular displacement is given by:

$$E = \frac{mg}{l} \frac{A^2}{2} \tag{1.5.3}$$

where m is the bob's mass, l the length of a pendulum, g represents acceleration of gravity and A characterises amplitude of displacement.

Since $mg/2l$ is the same for all cases shown in a figure 1.5.2, one gets, for the superposition of modes, the balance of energy:

$$(\tfrac{1}{2}A)^2 + (\tfrac{1}{2}A)^2 + (\tfrac{1}{2}A)^2 + (\tfrac{1}{2}A)^2 = A^2 \tag{1.5.4}$$

Similar balance holds for the potential energy of a spring, which is proportional to the square of its extension (or contraction). As long as superposition principle applies (small oscillation) the total energy is equal to the sum of the energies of the normal modes into which the motion can be decomposed.

Coordinates exhibiting the total energy as a sum over normal modes are called normal coordinates. If one assumes x_1 as a displacement of the pendulum 1 and x_2 as a displacement of the pendulum 2 those coordinates can be written as:

$$\zeta = \tfrac{1}{2} (x_1 + x_2) \tag{1.5.5a}$$

$$\eta = \tfrac{1}{2} (x_1 - x_2) \tag{1.5.5b}$$

Considering the general case when n is neither integral nor half-integral one can conclude that the motion will be strictly periodic if the frequencies f_{sym} and f_{asym} satisfy the condition:

$$\frac{p}{f_{sym}} = \frac{q}{f_{asym}} = \tau \tag{1.5.6}$$

where p and q are integers. In such a situation motion will repeat itself after time τ but return of energy will in general take a fraction of the time τ.

If f_{sym} / f_{asym} is not a rational number, motion of a system will not be strictly periodic.

When coupling is weak (a delicate spring) the value of n is large because n is inversely proportional to $(f_{asym} - f_{sym})$.

The time that elapses until the faster mode has gained a phase angle after n oscillations is given by:

$$nT_{sym} = n\frac{1}{f_{sym}} = \frac{1}{2(f_{asym} - f_{sym})} \qquad (1.5.7)$$

Thus energy will return to the first pendulum after a period that is twice so. This period - $2 \, nT_{sym}$ is called beat period. Denoting this as B one has:

$$B = 2nT_{sym} = \frac{1}{f_{asym} - f_{sym}} \qquad (1.5.8)$$

There is N beats in one second then:

$$N = \frac{1}{B} = f_{asym} - f_{sym} \qquad (1.5.9)$$

1.6. Wilberforce Pendulum

The Wilberforce pendulum was named for its inventor, Lionel Robert Wilberforce and represents an interesting case of coupled oscillations. The device consists of a helical spring of almost 2 meters and a cylindrical bob of the same radius. The bob has four vanes protruding from it and there is a nut on each of the vanes, which can be moved to change the moment of inertia of the system. Such a pendulum is illustrated in figure 1.6.1. which was found in [8]. It can be treated as a special case of the coupled oscillations of the longitudinal and the torsional modes for a mass hanging in a flexible helical spring.

A weak coupling is due to torsional strains coming from stretching and shrinking of the spring and the axial strains during twisting. When the frequencies of both modes are almost equal the energy of the system is transferred back and forth between these two modes.
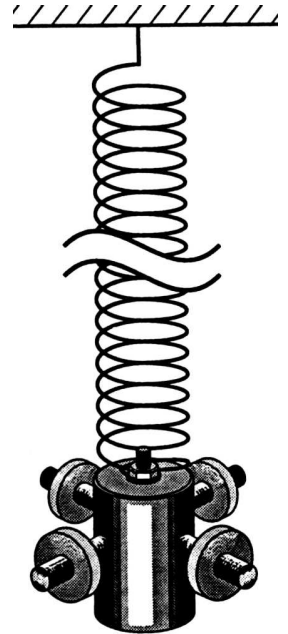

Figure 1.6.1. Silhouette of the Wilberforce pendulum

One can analyse analytically this phenomenon assuming there are two coordinates z - the vertical displacement of a bob and θ - the angle of its rotation and that in the equilibrium position $z=\theta=0$. If one considers a massless spring, with its longitudinal constant k and a torsional constant δ, to which a mass m, with a moment of inertia about its vertical axis I, has been attached and assumes a linear coupling of the form $\varepsilon z\theta/2$, the Lagrangian of the system has a form:

$$L = \tfrac{1}{2}m\dot{z}^2 + \tfrac{1}{2}m\dot{\theta}^2 - \tfrac{1}{2}kz^2 - \tfrac{1}{2}\delta\theta^2 - \tfrac{1}{2}\varepsilon z\theta \qquad (1.6.1)$$

Thus the equations of motion of Wilberforce pendulum are:

$$m\frac{d^2 z}{dt^2} + kz + \tfrac{1}{2}\varepsilon\theta = 0 \qquad (1.6.2a)$$

$$I\frac{d^2\theta}{dt^2} + \delta\theta + \tfrac{1}{2}\varepsilon z = 0 \qquad (1.6.2b)$$

As it has been already shown in paragraph 1.2 when the coupling does not take place one can observe simple oscillations.

In order to eliminate coordinate z from the equations of motion, one can solve the first of them for θ:

$$\theta = -\frac{2m}{\varepsilon}\cdot\frac{d^2 z}{dt^2} - \frac{2zk}{m\varepsilon} \qquad (1.6.3)$$

and using the values for the longitudinal and rotational frequencies:

$$\omega_z^2 = k/m \quad ; \quad \omega_\theta^2 = \delta/I \qquad (1.6.4)$$

get fourth order derivation equation of a form:

$$\frac{d^4\theta}{dt^4} + (\omega_z^2 + \omega_\theta^2)\frac{d^2\theta}{dt^2} + (\omega_z^2\omega_\theta^2 - \frac{\varepsilon^2}{4mI})\theta = 0 \qquad (1.6.5)$$

Assuming a solution to be:

$$\theta(t) = Ae^{i\omega\cdot t} \qquad (1.6.6)$$

one comes up with a bi-quadratic equation:

$$\omega^4 - (\omega_z^2 + \omega_\theta^2)\omega^2 + (\omega_z^2 \omega_\theta^2 - \frac{\varepsilon^2}{4mI}) = 0 \qquad (1.6.7)$$

By solving this formula frequencies of two normal modes can be calculated:

$$\omega_1^2 = \tfrac{1}{2}\{\omega_z^2 + \omega_\theta^2 - [(\omega_z^2 - \omega_\theta^2)^2 - \frac{\varepsilon^2}{mI})]^{\frac{1}{2}}\} \qquad (1.6.8a)$$

$$\omega_2^2 = \tfrac{1}{2}\{\omega_z^2 + \omega_\theta^2 + [(\omega_z^2 - \omega_\theta^2)^2 - \frac{\varepsilon^2}{mI})]^{\frac{1}{2}}\} \qquad (1.6.8b)$$

For $\omega_z = \omega_\theta = \omega$ they can be simplified to:

$$\omega_1^2 = \omega^2 + (\frac{\varepsilon^2}{4mI})^{\frac{1}{2}} \qquad (1.6.9a)$$

$$\omega_2^2 = \omega^2 - (\frac{\varepsilon^2}{4mI})^{\frac{1}{2}} \qquad (1.6.9a)$$

Being analogous to the situation described in paragraph 1.5. the values of ω_1 and ω_2 are close to each other and their difference $\omega_B = \omega_1 - \omega_2$ is the beat frequency between the two normal modes.

The general form of the rotation angle as a function of time will be a combination of the two normal modes:

$$\theta(t) = A\sin\omega_1 t + B\cos\omega_1 t + C\sin\omega_2 t + D\cos\omega_2 t \qquad (1.6.10)$$

when A, B, C, D are amplitudes of sine and cosine components of the modes.
Thus:

$$\dot{\theta}(t) = A\omega_1 \cos\omega_1 t - B\omega_1 \sin\omega_1 t + C\omega_2 \cos\omega_2 t - D\omega_2 \sin\omega_2 t \qquad (1.6.11)$$

$$\ddot{\theta}(t) = -A\omega_1^2 \sin\omega_1 t - B\omega_1^2 \cos\omega_1 t - C\omega_2^2 \sin\omega_2 t - D\omega_2^2 \cos\omega_2 t \qquad (1.6.12)$$

Using the equation of motion one gets general equation for z as a function of time in a form:

$$
\begin{aligned}
z(t) &= (2I\omega_1^2/\varepsilon)(A\sin\omega_1 t + B\cos\omega_1 t) \\
&+ (2I\omega_2^2/\varepsilon)(C\sin\omega_2 t + D\cos\omega_2 t) \\
&- (2/\delta)(A\sin\omega_1 t + B\cos\omega_1 t + C\sin\omega_2 t + D\cos\omega_2 t)
\end{aligned}
\tag{1.6.13}
$$

from which

$$
\begin{aligned}
\dot{z}(t) &= (2I\omega_1^3/\varepsilon)(A\cos\omega_1 t - B\sin\omega_1 t) \\
&+ (2I\omega_2^3/\varepsilon)(C\cos\omega_2 t - D\sin\omega_2 t) \\
&- (2/\delta)(A\omega_1\cos\omega_1 t - B\omega_1\sin\omega_1 t + C\omega_2\cos\omega_2 t - D\omega_2\sin\omega_2 t)
\end{aligned}
\tag{1.6.14}
$$

From the initial conditions,

$$
z(0) = z_0 \quad \dot{z}(0) = 0 \quad \theta(0) = \theta_0 \quad \dot{\theta}(0) = 0
\tag{1.6.15}
$$

where an initial vertical displacement and initial twist (but no initial velocity in either coordinate) are given, one can gain values for the amplitudes:

$$
A = C = 0
\tag{1.6.12}
$$

$$
B = (\omega_1^2 - \omega_2^2)^{-1}[\varepsilon z_0/2I - (\omega_2^2 - \omega_\theta^2)\theta_0]
\tag{1.6.13}
$$

$$
D = -(\omega_1^2 - \omega_2^2)^{-1}[\varepsilon z_0/2I - (\omega_1^2 - \omega_\theta^2)\theta_0]
\tag{1.6.14}
$$

Therefore the equations for both coordinates as functions of time have the form:

$$
\begin{aligned}
\theta(t) &= (\varepsilon z_0/2I)(\omega_1^2 - \omega_2^2)^{-1}(\cos\omega_1 t - \cos\omega_2 t) \\
&+ \theta_0(\omega_1^2 - \omega_2^2)^{-1}[(\omega_1^2 - \omega_\theta^2)\cos\omega_2 t - (\omega_2^2 - \omega_\theta^2)\cos\omega_1 t]
\end{aligned}
\tag{1.6.15}
$$

$$
\begin{aligned}
z(t) &= z_0(\omega_1^2 - \omega_2^2)^{-1}[(\omega_1^2 - \omega_\theta^2)\cos\omega_1 t - (\omega_2^2 - \omega_\theta^2)\cos\omega_2 t] \\
&- (2I\theta_0/\varepsilon)(\omega_1^2 - \omega_2^2)^{-1}(\omega_1^2 - \omega_\theta^2)(\omega_2^2 - \omega_\theta^2)\times(\cos\omega_1 t - \cos\omega_2 t)
\end{aligned}
\tag{1.6.16}
$$

The vector $\hat{X}$ describing the motion by such equations is a linear combination of the two normal modes with $\hat{z}$ describing longitudinal unit vector and $\hat{\theta}$ torsional unit vector:

$$\hat{X}(t) = z(t)\hat{z} + \theta(t)\hat{\theta} = A_1\hat{\eta}_1\cos\omega_1 t + A_2\hat{\eta}_2\cos\omega_2 t \qquad (1.6.17)$$

where $\hat{\eta}_1$ and $\hat{\eta}_2$ are the normal coordinates of the form:

$$\hat{\eta}_1 = \hat{\theta} + (2I/\varepsilon)(\omega_1^2 - \omega_\theta^2)\hat{z} \qquad (1.6.18a)$$

$$\hat{\eta}_2 = \hat{\theta} + (2I/\varepsilon)(\omega_2^2 - \omega_\theta^2)\hat{z} \qquad (1.6.18b)$$

Also from equations (1.6.9) the coupling constant can be calculated:

$$\varepsilon = (\omega_1^2 - \omega_2^2)\sqrt{mI} \qquad (1.6.19)$$

1.7. Fourier analysis

A mathematical technique known as Fourier analysis can be used to represent any function *f(x)* (where *x* may be position or *time*) as a series of periodic functions that is called Fourier series and can be written as:

$$\text{F(x)} = \tfrac{1}{2}\,a_0 + a_1\cos x + a_2\cos 2x + \ldots + a_n\cos nx$$

$$+ b_1\sin x + b_2\sin 2x + \ldots + b_n\sin nx + \ldots = \qquad (1)$$

$$\tfrac{1}{2}\,a_0 + \sum_{n=1}^{\infty} a_n\cos nx + \sum_{n=1}^{\infty} b_n\sin nx$$

The series consists a constant term $\tfrac{1}{2}a_0$ and sum of sine and cosine terms of different amplitudes a_n, b_n. The frequencies of the trigonometric functions are harmonics of the fundamental frequency of *x*. To represent a certain waveform by Fourier series values of the coefficients have to be determined by integration of *f(x)* over period 2π with formulas:

$$a_n = \frac{1}{\pi}\int_0^{2\pi} f(x)\cos nx\, dx \qquad (2)$$

$$b_n = \frac{1}{\pi}\int_0^{2\pi} f(x)\sin nx\, dx \qquad (3)$$

The first term can be obtained by solving:

$$a_0 = \frac{1}{2\pi} \int_0^{2\pi} f(x)\,dx \qquad (4)$$

With use of Fourier analysis fundamental frequencies of signals can be determined. Exact formulas for coefficients vary for different functions $f(x)$ (periodic, nonperiodic function, wave packet) being analyse [9].

Chapter 2. Creating Video Clips, Preparing to Measure and Analysing Results

2.1. Setting up Experiments and Recording Video Clips

Real experiments on motion of Wilberforce pendulum were carried out with the same device as described in [1]. The figure 2.1.1 illustrates such a pendulum which contains:

- a spring of 17 turns of a steel wire with radius $r=7,25 \times 10^{-4}$ m whose unloaded length is equal to $l_0=1,30 \times 10^{-1}$ m and projected radius of the helix is $R_s=2,60 \times 10^{-2}$ m; and whose mass is $m_s=3,43 \times 10^{-2}$ kg,

- a cylindrical bob with a radius $R_b=3,50 \times 10^{-2}$ m and mass $m=4,3032 \times 10^{-1}$ kg that contains two vanes protruding from it on which identical, free-to-move, nuts are located.
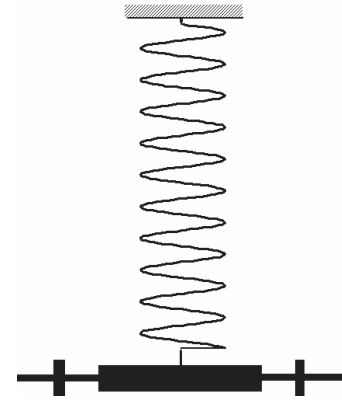
Figure 2.1.1 Silhouette of a used pendulum

Basing on founding about resonance of longitudinal and torsional oscillations reported in [1], experiments were done for the pendulum with its nuts placed symmetrically at a distance $\Delta R = 3,50 \times 10^{-2}$ m from the edge of a bob which corresponds to a value of a moment of inertia $I = 0,000335$ kgm^{-2} and with different combinations of the initial conditions determined by the longitudinal displacement z_0 and an angle of twist of a bob θ_0. These combinations are presented in table 2.1.1.

Table 2.1.1. Combination of the initial conditions

experiment's number	initial conditions	
	z_0 [m]	θ_0 [rad]
1	0.04	0
2	0.04	$\pi/2$
3	-0.04	0
4	-0.04	$-\pi/2$
5	0	$-\pi/2$
6	- 0.04	$\pi/2$
7	0	$\pi/2$
8	0.04	$-\pi/2$

Experiments were carefully set up in a way that allows placing a video camera under the pendulum's bob as well as in front of it. Special attention has been given to background and lighting.

For each set of initial conditions a number of one-minute clips of Wilberforce pendulum motion from both camera perspectives has been recorded, using a *Sony*® digital video camera *DCR-TRV 8E*. Specific information about the camera and its features can be found in [10].

All digital movies were carefully viewed on a big screen and the best one for every set of initial conditions has been chosen for further processing. Approximately 1200 captured frames for every combination of z_0 and θ_0 with a program for video editing were used.

2.2. Editing Digital Movies with AdobePremiere

AdobePremiere is an advanced program for creating and editing digital movies. It allows capturing and performing necessary processing (cutting, adding transitions, titles, motion, transparency etc.). After processing with the program a final clip can be produced in various formats. More information about the program and its features can be found [11].

To prepare video clips for data video measurement only a few simple processing acts have been performed. After capturing, each movie was cut to consist of 1025 frames presenting motion of the pendulum. Every movie was also cropped to reduce its size from 768×576 pixels (PAL standard) to a size shown in table 2.2.1. Because during process of covering a digital camera interlaces movie's frames as a last an operation of deinterlacing was proceeded. Finally all video clips were converted into an *.avi format. The table 2.2.1 contains information about both kinds of movies made with a different camera perspective.

Table 2.2.1. General information about video clips

camera perspective	bottom	face
frame width	380 pixels	480 pixels
frame height	380 pixels	320 pixels
frame length	41 sec	41 sec
frame count	1025	1025
frame rate	25 per sec	25 per sec
average size	41 Mb	42 Mb
video compression	Cinepak Codec	Cinepak Codec

The figure 2.2.1a presents a first frame of a movie covered from the bottom and consisting of motion of the pendulum that has been released with initial longitudinal displacement $z_0 = 0.04\ m$ and initial rotational angle $\theta_0 = 0$. The figure 1b shows a first frame of a movie done from front perspective and with the same initial conditions.
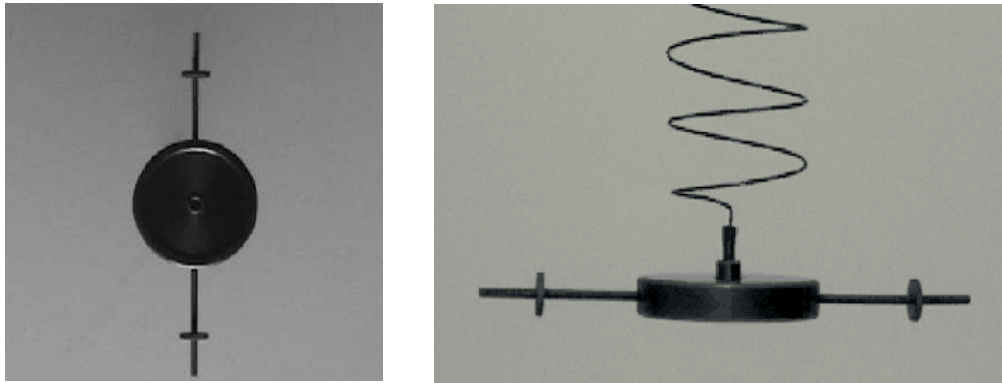
Figure 2.2.1. First frames of video clips taken: a) from the bottom b) from the front
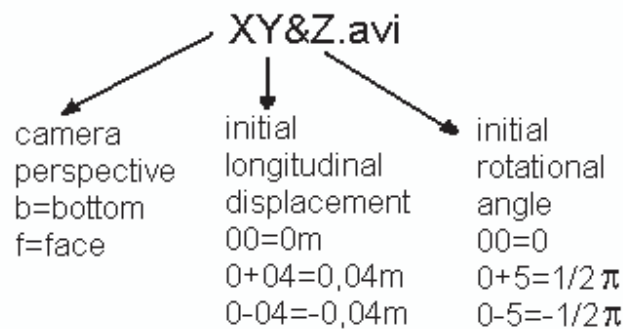

Figure 2.2.2. An explanation of a movie file name

All movies (*.avi files) are recorded on 2 CDs (Wilberforce_b and Wilberforce_f) and enclosed in the thesis. Figure 2.2.2. explains names that have been given to them.

2.3. Program Coach 5 and Data Video

Coach 5 is an integrated software package developed by the CMA Foundation of the University of Amsterdam. The program is an open environment for investigation in science and technology and integrates measuring, data analysis and processing, modelling, controlling and video measuring. Only the last mode of the program – Data Video – is essential for the present case and will be described in depth.

Video measurement allows collecting data from digital video clips in form of points that consist of x, y coordinates of a monitored element taken at certain *time*. The location of the item of interest is marked by clicking on its position in chosen frames of the whole movie. The

program supports *.avi and *.mov digital video formats. Although Coach 5 allows plotting data in graphs, viewing and calculating new quantities in tables and performing analysis, obtained data were exported from the program as a *.dif file.

Further mathematical elaboration was carried out with a Microsoft® Excel 97 spreadsheet.

To proceed with video measurement one has to determine:

- a scaling factor – the distance on the movie frame that corresponds to actual (real life) distance,

- a location of the axis for future measurements,

- a setting of the origin,

- a time calibration by noting the rate (x/per second) with which the processing movie has been made.

All those requirements have been taken into account during the process of preparation of a movie to be measured and therefore:

- as a scaling factor a value of a bob's diameter has been used,

- movies were covered with a rate of 25 frames per second,

- information about a location of the origin and measurement procedure is described in the next chapter.

Specific information about Data Video mode of Coach 5 can be found in [12]. Examples of Data Video activities are provided in [13].

2.4. MS Excel and its Fast Fourier Transform

Program Microsoft® Excel is used to calculate, analyze and plot results of video measurements. Data is mathematically calculated in Excel spreadsheet and results are plotted in separate sheets. A data analysis tool – Fourier analysis that uses fast Fourier transform (FFT) – is applied to time domain data $z=f(t)$ or $\theta=f(t)$ to find their components. As a result of such a transformation a set of complex numbers – frequency domain output is gained.

Fourier transform is based on the principle that any function can be represented as a superposition of sinusoidal components with certain amplitude.

A frequency step in Excel FFT is indicated by the number of measured point which has to be an even number power of 2 and amplitude is obtained from an absolute value (modulus) of a

complex number. These are displayed as a graph of amplitudes of the components against their frequencies. Such a graph is called a spectrum.

Chapter 3. The Experiments and Results

3.1. The Experiments

The video measurements were carried out with aid of the program Coach 5.

On the series of 8 clips with a motion of Wilberforce pendulum viewed from its front the measurements of bob's position on each frame were taken. The data, obtained by marking with Coach 5 Data Video mode a certain point on the device, contained 1024 triplets of *time* and position coordinates *x* and *y*. Only the pieces of information on *y* as a function of *time* were exported as a *.dif files and analyzed later on. Figure 3.1.1 shows a part of Data Video window with a frame of a movie with a measured point. Also an axis and a scaling factor are shown.

On the next 8 clips, taken from the bottom of the pendulum, measurements of a position of the nut on a pendulum's vanes have been taken. They also contained 1024 triplets of *time* and position coordinates *x* and *y*. According to the fact that an origin of the coordinate system was marked in the center of the pendulum, a rotation angle was mathematically calculated from both *x* and *y* coordinates. Figure 3.1.2 presents a part of Data Video window with a frame of a movie with a measured point, an axis and scaling factor.

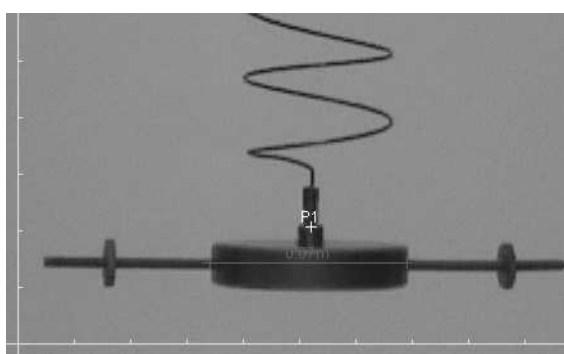To present all finding and carry on calculations a Microsoft® Excel 97 spreadsheet was used.

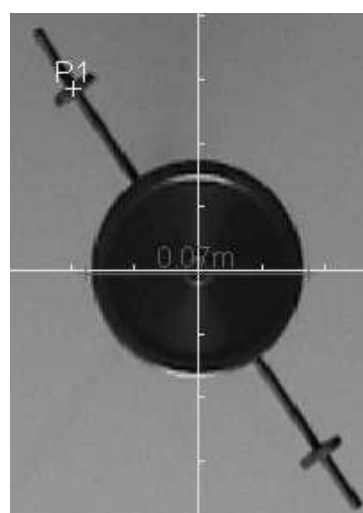Figure 3.1.1. A part of a Data Video window for a movie recorded from the front

Figure 3.1.2. A part of a Data Video window for a movie recorded from the bottom

3.2. Statements of Experimental Results

The table 3.2.1 presents a part of a Microsoft® Excel spreadsheet table in which data has been mathematically elaborated.

The first column contains an *index* number, which is the same as a number of a frame on which the measurement took place. The next column contains *time* related to a frame at which a value of *y* was determined in a certain video clip.

Because the axis was set as the same for every frame the quantity calculated with use of a formula:

$$y_n - y_{average}$$

represents vertical displacement of the pendulum bob *z*. An average value of *y* that represents an equilibrium position of a bob is shown in a fourth column. The next column of the table encloses values of displacement *z*.

On those results a fast Fourier transformation has been performed. The result of the procedure – a set of complex numbers – is presented in the sixth column. Information about amplitude of a certain frequency component is indicated by the absolute value (modulus) of those complex numbers. Those values are presented in eighth column, which is preceded by a column that shows values of frequencies. To normalise amplitudes, corresponding to Fourier analysis to unity a maximum value of this quantity has been determined and used to create the last column of the table according to an equation:

$$A_{nor}^n = \frac{A_n}{A_{max}}.$$

Table 3.2.2 contains data and calculated results related to the second coordinate, the angle of rotation *θ*. Similarly to the first table three first columns enclosed *index*, *time* and *y*. The next one presents information about *x* position component of the location of a bob's nut. The origin has been placed on every frame in a centre of a bob so its rotation angle can be calculated from *x* and *y* with use of trigonometry. Therefore the value of *c* - hypotenuse

Figure 3.2.1. Coordinates x, y and c for video clips covered from the bottom

in a triangle shown in a figure 3.2.1 has been determined and presented in a fifth column.

To calculate an angle a following if-and-statement has been used:

IF {AND (y<0,x<0), 2·π - ACOS(y/c), IF [AND (y>0,x<0), -ACOS(y/c), ACOS(y/c)]}

Such a formula was used to overcome difficulties that appear when function arctangent was used for angles outside the range $[0,\pi]$.

Results of the calculations are contained in a sixth column of the table 3.2.2 and were used to obtain the average value of the angle that represents an equilibrium position of a bob (placed in the next column). A formula:

$$\alpha_n - \alpha_{avrage}$$

allows calculating the second coordinate – torsional displacement of the pendulum bob θ. This information is presented in the eighth column. Similarly to the first table next columns consist of information about the results of the fast Fourier transformation, amplitudes of certain frequency components, maximum amplitude and normalised amplitudes.

Based on the calculations a number of diagrams have been drawn. Diagrams 3.2.1 to 3.2.16 with even numbers present vertical displacement z as a function of time for different initial condition while those of odd numbers illustrate Fourier spectrum for *z(t)*. The diagrams 3.2.17 to 3.2.32 with even numbers present rotation angle θ as a function of time for different initial condition while those of odd numbers illustrate Fourier spectrum for *θ(t)*.

Values of frequencies of modes *f₁=1,031 [Hz]* and *f₂= 0.982 [Hz]* where then used to calculate a frequency of a produced 'tone', a beating rate and the coupling constant (formula (19) in paragraph 1.6.) which were found to be:

$$f_t=1/2(f_1+ f_2)=1,007[Hz]$$
$$f_b= f_1- f_2=0,049[Hz]$$
$$\varepsilon = 0,046 \ [kg \cdot m \cdot rad/ s]$$

3.3. Some Consideration of Video Measurement Accuracy

Establishing accuracy for video measurement is problematic because it is not a commonly used method. The accuracy of such a measurement is mainly determined by the quality of a movie (focus) and its size (resolution).

During a process of scaling both kinds of movies, the number of pixels indicating a real length has been measured to be:

- for the video clip taken from bottom perspective:

  $125pix = 7,0 \times 10^{-2}$ m ($1pix = 5,6 \times 10^{-4}$ m),

- for the video clip taken from face perspective:

  $155pix = 7,0 \times 10^{-2}$ m ($1pix = 4,5 \times 10^{-4}$ m).

It has been experimentally checked that the movie of dimensions 380×380 pixels presented in a full size on a computer screen of 17", with a resolution 1024×768 has a length $l = 2,00 \times 10^{-1}$ m. The resolution of movies and their focus allows locating a certain point with accuracy ±2 pixels which on such a screen is equal to $\Delta l = \pm 1,3 \times 10^{-3}$ m. Therefore estimated accuracy of the video measurement from a movie is:

- for the video clip taken from front perspective (one marked point on every frame):

  $\Delta y = \pm 0,9 \times 10^{-3}$ m

- for the video clip taken from bottom perspective (a point and axis marked on every frame): $\Delta y = \Delta x = \pm 2,2 \times 10^{-3}$ m.

According to accuracy of a position and a fact that a frequency step of fast Fourier transformation depends on a number of measured points the accuracy for frequency has been estimated as:

- for the video clip taken from face perspective: $\Delta f = \pm 0,025$ Hz,
- for the video clip taken from bottom perspective: $\Delta f = \pm 0,05$ Hz.

3.4. Conclusions

Video measurements of motion of the Wilberforce pendulum allowed observing both types of the coupled oscillations, longitudinal and torsional ones. Visualization of the torsional oscillations is especially interesting, as in the previous paper [1], where ultrasonic sensor was used instead of a video camera and only the longitudinal oscillations were observed. All experiments in this paper were carried out for the cases of resonance between both kinds of oscillations. Fourier analyses of the results have revealed presence of one or two normal modes in each type of oscillations. According to motion of coupled pendulums, shown in the figure 1.5.1 the normal modes of the Wilberforce pendulum are obtained for certain initial conditions corresponding to releasing the coupled pendulums in the same phase (first mode) or in anti-phase (second mode). Table 3.4.1 summarises location of the peaks of frequency in spectrums.

Table 3.4.1. Frequency values for peaks in spectrums

Experiment's number	initial conditions		face perspective		bottom perspective	
	z_0 [m]	θ_0 [rad]	f_1 [Hz]	f_2 [Hz]	f_1 [Hz]	f_2 [Hz]
1	0.04	0	0.982	1.031	0.982	1.031
2	0.04	$\pi/2$	-	1.031	-	1.031
3	-0.04	0	0.982	1.031	0.982	1.031
4	-0.04	$-\pi/2$	-	1.031	-	1.031
5	0	$-\pi/2$	0.982	1.031	0.982	1.055
6	- 0.04	$\pi/2$	0.982	-	0.982	-
7	0	$\pi/2$	0.982	1.031	0.982	1.055
8	0.04	$-\pi/2$	-	1.031	0.982	-

The first mode is visible as a dominating in the experiment 6 when the spring is pulled downwards and wound more tightly (figure 3.2.15, 3.2.16, 3.2.31, 3.2.32) and in the experiment 8 when the spring is lifted and unwound (figures 3.2.11, 3.2.12, 3.2.27, 3.2.28). The second mode is dominant in experiment 4 when the spring is pulled downwards and unwound (figure 3.2.7, 3.2.8, 3.2.19, 3.2.20) and in the experiment 2 when the spring is lifted and wound (figure 3.2.3, 3.2.4, 3.2.23, 3.2.24). Because it is very difficult to set the pendulum in motion very accurately, for almost all cases the other mode is noticeably present but its amplitude is very small.

For the rest of the experiments (1, 3, 5, 7) the beats of both modes are observable. It is indicated by almost the same (or close) value of the amplitudes corresponding to the two

modes in the spectrum (figure 3.2.1, 3.2.2, 3.2.5, 3.2.6, 3.2.9, 3.2.10, 3.2.13, 3.2.14, 3.2.17, 3.2.18, 3.2.21, 3.2.22, 3.2.25, 3.2.26, 3.2.29, 3.2.30).

For measurements done on video clips covered from a face perspective (longitudinal oscillations) all peaks of frequency in spectrums are observed when $f_1 = 0,982[Hz]$ and $f_2 = 1,031[Hz]$. The same results, within experimental accuracy, are gained for torsional oscillations. The average frequency $f_t = 1,006[Hz]$ ('tone' frequency) and the beating rate $f_b = 0,049[Hz]$ are in agreement with theoretical values for case of resonance ($f_1 = f_2 = 1,01[Hz]$) and results presented in [1].

The results allowed calculating the value of coupling constant and confirm that the assumption about the linear coupling used when writing the motion equations (1.6.2a-b) is valid.

An increase of accuracy can be obtained by enlarging a number of measured points or/and a size of a video movie (its width and height). This changes cost increase of time for taking date and size of a movie (in Mb).

IV. Closing Remarks

The use of digital techniques seems to be useful and powerful tool for (re)investigation of various phenomena. Although it requires considerable work to prepare a movie and special processing to make measurements, it is still worth doing. The fact that once produced the movie which can be copied and used by many investigators encourages taking advantage of such a measurement. Especially having in mind the growing number of computers that are used in education at the secondary and university level it indicates one new future use of ICT in schools.

Use of a data video measurement allows students to go with their interest outside of school. It can also be used to explore and analyze many aspects of motion in everyday life.

The present study shows that already existing programs such as Coach 5, AdobePremiere and Excel can be used with great success in the field of scientific investigation. It also points out that an increase in accuracy of data video and decrease in time necessary to take measurements would be welcome especially when the number of video points is large. This can be obtained by automating the data collection process. Therefore a procedure of automatically recognising and marking a characteristic point on every frame (for example one certain colour) could be implemented into a program.

Nevertheless also more complicated examples of motion and aspects related to it can be investigated with use of data video. An example of such an interesting problem for further consideration can be a study on motion of a human body.

V. Literature

1. Ewa Dębowska, Stanisław Jakubowicz, Zygmunt Mazur, *Computer visualization of the beating of a Wilberforce pendulum,* European Journal of Physics **20**, 89-95, 1999

2. Henryk Szydłowski, *Pracownia fizyczna,* PWN, Warszawa 1973

3. Michael Mansfield, Colm O'Sullivan, *Understanding Physics,* Johan Wiley & Sons, Chichester 1998

4. Ernessto E. Galloni, Mario Kohen, *Influence of the mass of the spring on its static and dynamic effects,* American Journal of Physics **47** 1076-8, 1979

5. Ronald Geballe, *Statics and Dynamics of a Helical Spring,* American Journal of Physics **26** 287-90, 1957

6. Arnold Sommmerfeld, *Mechanics of Deformable Bodies: Lectures on Theoretical Physics vol. II,* New York Academic, 1964

7. Joseph Aharoni, *Lectures on mechanics: for students of physics and engineering,* Oxford University Press, Oxford 1972

8. Richard E. Berg, Todd S. Marshall, *Wilberforce pendulum oscillations and normal modes,* American Journal of Physics **59**, 32-8, 1991

9. Frank S. Crawford, Jr., *Berkeley Physics Course – vol III, Waves,* Mcgraw-hill Book Company, Berkeley 1968

10. *Manual of Digital Video Camera Recorder,* Sony Corporation 1999

11. *Adobe®Premiere®5.1 User Guide,* Adobe System Incorporated 1998

12. *Guide to Coach 5,* CMA/Amstel Institute, Amsterdam 2000

13. Ewa Mioduszewska, *Coach System Workbook,* CMA/Amstel Institute, Amsterdam 2000

VI. Acknowledgements

Thanks

I would like to thank my promotor prof. Ewa Dębowska for her valuable remarks and comments during development of the thesis. I also thank dr. William Wehrbein who checked the paper from a language standpoint and gave me quite an English lesson.

Special words of appreciation are addressed to my program co-ordinator dr. Ton L. Ellermeijer and all workers of Amstel Institute who helped, supported and encouraged me during my study at University of Amsterdam.

This thesis could not have been written without a support from my Parents whom I owe all of my education.

Last but not least, I thank Jola for her persistence and patience.

Podziękowania

Składam wyrazy podziękowania Pani promotor, prof. Ewie Dębowskiej, za cenne uwagi oraz komentarz podczas tworzenia niniejszej pracy. Dziękuję także dr. Willamowi Wehrbein, który podjął się korekty językowej pracy i udzielił mi cennych lekcji angielskiego.

Szczególne słowa podziękowania kieruję do dr. Tona L. Ellermeijera oraz pracowników Instytutu Amstel za ich pomoc, zrozumienie i wsparcie podczas mojego pobytu na Uniwersytecie w Amsterdamie.

Praca ta nie powstałaby bez pomocy i wsparcia moich Rodziców, którym dziękuje za wszystkie lata spędzone w szkole.

Dziękuję również Jolancie za jej wytrwałość i cierpliwość.